Available online at www.sciencedirect.com
SCIENCE DIRECT®
Journal of Organometallic Chemistry 664 (2002) 161–169
Journal of Organometallic Chemistry
www.elsevier.com/locate/jorganchem

Cyclic thioether and acyclic thioether–thiolate complexes of pentamethylcyclopentadienyl ruthenium(II, III)

Lai Yoong Goh *, Ming Ern Teo, Soo Beng Khoo, Weng Kee Leong, Jagadese J. Vittal

Department of Chemistry, National University of Singapore, Kent Ridge, Singapore 119260, Singapore

Received 1 August 2002; received in revised form 1 August 2002; accepted 20 September 2002

Abstract

The reaction of $[Cp^*RuCl_2]_2$ (**7**) ($Cp^* = \eta^5$-C_5Me_5) with $S(CH_2CH_2S^-)_2$ (tpdt) and trithiacyclononane (9S3) gave the monomeric complexes Cp*Ru(tpdt) (**6**) and $[Cp^*Ru(9S3)](PF_6)$ (**8**) as dark purple and yellow crystals, respectively. Treatment of **6** with **7** and $[(C_6Me_6)RuCl_2]_2$ (**2**) led to the isolation of Ru–Ru bonded complexes $[Cp^*Ru(tpdt)(Ru(Cl)Cp^*](PF_6)$ (**9**) and $[Cp^*Ru(tpdt)(Ru(C_6Me_6)](PF_6)$ (**10**) as dark red and purple crystals, respectively. The complexes, **6** and **8**–**10** have been spectrally and structurally characterized.

Keywords: Ruthenium; Thiolate–thioether; Pentamethylcyclopentadienyl; 3-Thiapentane-1,5-dithiolate; Structures

1. Introduction

Transition metal complexes with sulfur-based ligands are of continuing interest as models for biological systems and industrial metal sulfide catalysts [1]. However, whereas the coordination chemistry of mono- and bi-dentate thiolates have been extensively studied [2], metal complexes (**1**) (Fig. 1) of the tridentate 3-thiapentane-1,5-dithiolate ligand, $S(CH_2CH_2S^-)_2$ (tpdt), containing both thioether and thiolate sulfur atoms, are rather limited, being largely found only among the radiopharmaceutically-significant compounds of Re and Tc [3–7], and a few examples of complexes of In [9] and Sb [10].

Ligated tpdt has been formed by ligand coupling of ethane-1,2-dithiolate at Nb and Ta (Eq. (i)) [11], and cleavage of an ethene (C_2H_4) unit from a trithiacyclononane (9S3) ligand initiated by an L-ascorbic acid reduction of a 9S3 complex (Eq. (ii)) [8]. We have recently prepared $[(C_6Me_6)Ru(tpdt)]$ (**3**) from the reaction of $[(C_6Me_6)RuCl_2]_2$ (**2**) with $Na_2(tpdt)$ (Eq. (iii)), and found that **3** underwent ring closure with dibromoalkanes, $Br(CH_2)_nBr$ ($n = 1$–5) to generate trithiathioether complexes $[(C_6Me_6)Ru(z\text{S}3)]^{2+}$ ($z = 8$–12) (**4**) (Eq. (iv)) [12], which is reminiscent of Sellmann's template alkylation reaction at $[Mo(CO)_3(tpdt)]$ in the synthesis of 9S3 [13]. The thiolate sulfur atoms of **3** readily bridge a second Ru centre to generate a binuclear cationic complex $[\{(\eta^6\text{-}C_6Me_6)Ru\}_2Cl(\mu\text{-}\eta^2,\eta^3\text{-}C_4H_8S_3)]Cl$ (**5**) (Eq. (v)) [12]. We were therefore interested to investigate the related chemistry of the Cp* analogue of **3**, viz. [Cp*Ru(tpdt)] (**6**). The results are described below.

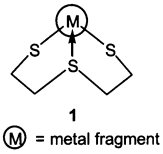

1

Ⓜ = metal fragment

Fig. 1. Metal complexes of tpdt.

* Corresponding author. Tel.: +65-687-42677; fax: +65-677-91691
E-mail address: chmgohly@nus.edu.sg (L.Y. Goh).

0022-328X/02/$ - see front matter © 2002 Elsevier Science B.V. All rights reserved.
PII: S0022-328X(02)01977-0

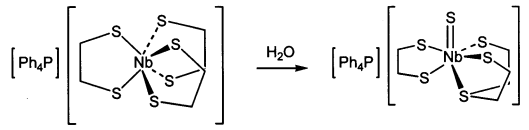

.....(i)

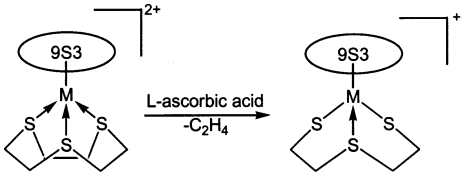

.....(ii)

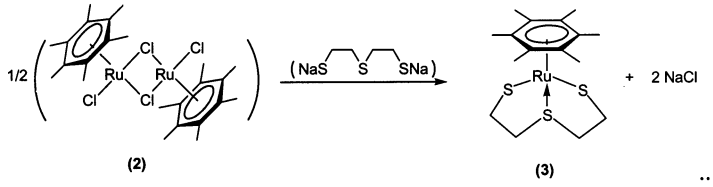

.....(iii)

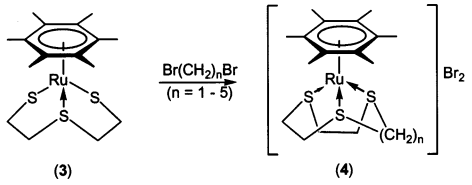

.....(iv)

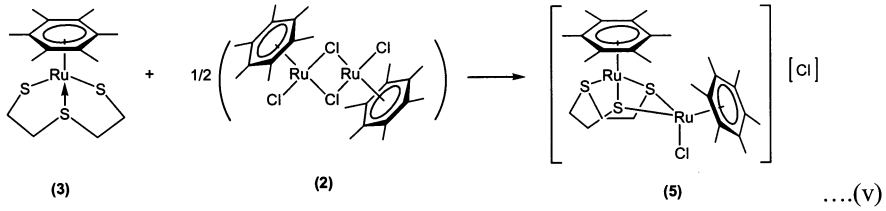

....(v)

2. Results and discussion

2.1. Synthesis and spectroscopic data

2.1.1. Preparation of [Cp*Ru(tpdt)] (6) and [Cp*Ru(9S3)] (PF_6) (8)

[Cp*Ru(tpdt)] (**6**) was obtained as lustrous purplish black needles in 57% yield from $[Cp^*RuCl_2]_2$ (**7**), via a method successfully utilized for the preparation of the C_6Me_6 analogue **3**, as illustrated in Eq. (iii). Unlike in the case of **3** [12], the dithiolate ligand in **6** does not undergo alkylation with dibromoethane to generate a 9S3 complex [Cp*Ru(9S3)]Br. Perhaps this is not surprising since such a reaction of **6** will involve the reduction of Ru(III) to Ru(II), which we attempted to achieve in the presence of metallic zinc without success. However, we were able to obtain this compound as its PF_6^- salt (**8**) in 57% yield via the labile tris–acetone complex obtained by the reaction of **7** with $AgPF_6$ in acetone (Eq. (vi)), a method previously employed for the synthesis of $[(C_6Me_6)Ru(9S3)](PF_6)_2$ (**4A**) [14]. While this work was in progress Grant et al. [15] reported the synthesis of the Cp analogue of **8**, viz. $[CpRu(9S3)](PF_6)$ (**8A**) via an alternative route shown in Eq. (vii).

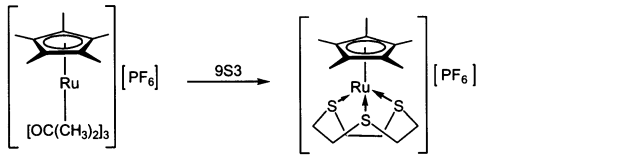

(8) ……..(vi)

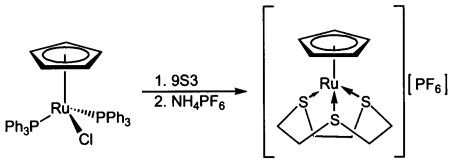

(8A) …….(vii)

2.1.2. Reaction of **6** with μ-dichloro-diruthenium complexes

An ambient temperature reaction of **6** with $[Cp^*RuCl_2]_2$ (**7**) produced the diruthenium complex $[Cp^*Ru(tpdt)Ru(Cl)Cp^*](PF_6)$ (**9**) as dark red solids in 68% yield, after metathesis with NH_4PF_6 (Eq. (viii)). A similar reaction with $[(C_6Me_6)RuCl_2)_2]$ (**2**) yielded $[Cp^*Ru(tpdt)Ru(C_6Me_6)](PF_6)$ (**10**) as purplish red solids in 25% yield (Eq. (ix)).

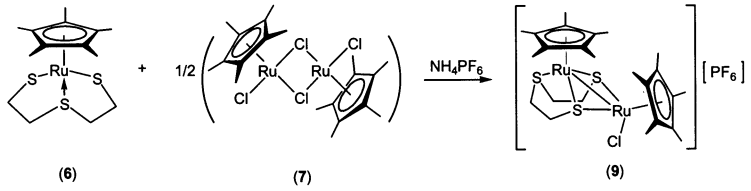

(6) (7) (9) ……..(viii)

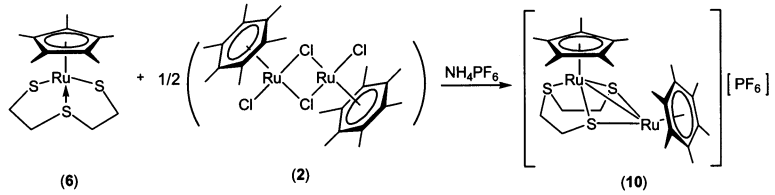

(6) (2) (10) ……..(ix)

2.2. Spectroscopic data

The ^{1}H-NMR spectrum of **6** exhibits variable-temperature behaviour. At 300 K, two broad peaks are observed at δ −0.10 ($\nu_{1/2}$ ca. 50 Hz) and −3.15 ($\nu_{1/2}$ ca. 200 Hz), which are assigned to the methylene and Cp* protons, respectively, on the basis of their relative intensities. In the temperature range 300–253 K, the first peak shifts from δ −0.10 to −1.81 with increasing broadening ($\nu_{1/2}$ ca. 50–600 Hz) till it eventually merges into the baseline below 250 K. The second peak undergoes a similar shift from δ −3.15 to −5.1 at 233 K, with similar broadening and disappearance by 213 K. Anomalous chemical shifts and such temperature-dependent variations in chemical shifts and line-broadening are often encountered in paramagnetic systems [16], of which this d^5-Ru(III) compound **6** is an example. The FAB mass spectrum shows the parent ion at m/z 389.

In the ^{1}H-NMR spectrum of **8**, the methyl groups on the Cp* ring are observed as a singlet at δ 1.78 and the methylene protons as a multiplet centred at δ 2.41, consisting of two overlapping mutiplets, possessing an ABCD pattern (J ca. 18 Hz), characteristic of 9S3 ligands coordinated to a metal centre [17]. The resonance of the methylene protons of the complexes shifts towards lower field as follows: **8** (δ 2.41) > **4** (δ 2.78) [18] > $[Ru(9S3)_2]^{2+}$ (δ 2.9–3.0) [19], in agreement with the increasing electron-donating ability of the coligand (9S3 < C_6Me_6 < Cp*), which will result in increasing shielding of the ligand protons in the order ($[Ru(9S3)_2]^{2+}$ < **4** < **8**). The ^{13}C-NMR spectrum of **8** shows signals for the methylene carbons at δ 34.1 and for the Cp* ring and methyl carbons at δ 91.2 and 9.9, respectively.

The FAB^+-mass spectrum of **8** shows the parent ion at m/z 417, while the FAB^--mass spectrum indicates

the presence of the counter ion PF_6^-. This is supported by the IR spectrum, which shows strong bands at 840 and 557 cm^{-1} pertaining to P–F stretching frequencies.

The NMR spectra of **9** are consistent with the presence of two inequivalent Cp* rings, the Me resonances of which are seen at δ 1.65 and 1.88 in the ^1H spectrum and at δ 10.0 and 10.7 in the ^{13}C spectrum, which also shows the ring carbons at δ 101.2 and 102.4. The methylene protons of the thiolato ligand are seen as two clusters of multiplets centered at δ 2.74 and 3.04 (relative intensity 1:1) in the ^1H spectrum and as singlets at δ 37.4 and 41.6 in the ^{13}C spectrum, in agreement with the presence of a mirror plane of symmetry containing Ru(1), Ru(2) and S(2) in the molecule. The ESI^+-mass spectrum shows the parent ion at *m/z* 661.

The ^1H NMR spectrum of **10** possesses two sharp singlets at δ 1.72 and 2.25, assignable to the methyl protons on the Cp* and C_6Me_6 ligands, respectively, on the basis of their relative integrals. The methylene proton peaks are seen as multiplets at δ 0.75, 1.92 and 3.03–3.27. The ^{13}C resonances are observed at δ 6.1 and 12.8 for the Me groups and at δ 88.7 and 91.0 for the arene and Cp* ring carbon atoms, respectively. The ESI^+-MS of **10** shows the presence of the parent cation at *m/z* 653 and successive losses of ethylene fragments to give mass peaks at *m/z* 625 [$Cp^*Ru(S(CH_2)_2S_2)$-$Ru(C_6Me_6)$] and 596 [$Cp^*RuS_3Ru(C_6Me_6)$], followed by further cleavage of a sulfur atom and a Cp* ligand to give mass fragments *m/z* 564 [$Cp^*RuS_2Ru(C_6Me_6)$] and *m/z* 434 [$RuS_2Ru(C_6Me_6)$], respectively. The ESI^- mass spectrum indicates the presence of the PF_6 anion at *m/z* 145. This is supported by the IR spectrum which exhibits the characteristic strong P–F bond stretching frequencies at 839 and 557 cm^{-1}.

2.3. Electrochemical study of 8

A cyclic voltammetric study of **8** was carried out to compare its relative stability to oxidation with that of the Cp analogue and that of the homoleptic $[Ru(9S3)_2]^{2+}$ analogue. The voltammogram shows a reversible oxidation wave with an E° value of +713 mV versus Ag/Ag^+ reference (+516 mV vs. the ferrocene/ferrocenium couple) [20], as compared with +966 mV for the Cp analogue [15] and +1410 mV for $[Ru(9S3)_2]^{2+}$ [21] (measured vs. ferrocene/ferrocenium), indicating a slightly higher stability to oxidation than the Cp analogue.

2.4. Structural studies

The molecular structures of [Cp*Ru(tpdt)] (**6**), [Cp*Ru(9S3)](PF_6) (**8**), [Cp*Ru(tpdt)Ru(Cl)Cp*](PF_6) (**9**) and [Cp*Ru(tpdt)Ru(C_6Me_6)](PF_6) (**10**) have been determined by single-crystal X-ray diffraction analysis. The crystallographic data for all four complexes are given in Table 1, and the molecular structures are shown in Figs. 2–5. Selected bond parameters of these compounds are given in Table 2 together with those of analogues for comparison.

The mononuclear complexes, **6** and **8**, possess the piano-stool configuration at Ru; the 9S3 ligand in **8** is coordinated to Ru(II) in its normally-encountered confacial tridentate coordination mode. As in the case of the homoleptic $[Ru(9S3)_2]^{2+}$ complex, the molecule of **8** possesses a plane of symmetry formed by C(1), C(10), Ru(1) and S(2), as reflected in the bond parameters. The Cp* ring and the plane of the S atoms of 9S3 are tilted with respect to each other; the deviation/tilt of 0.029 Å for the Cp* ring is much larger than that reported (0.005 Å) for the Cp ring in [CpRu(9S3)](PF_6) (**8A**). This feature is reflected in the smaller distance of the Cp* corners C(3) and C(3)#1 and S(2) from the Ru centre than the other members of the Cp* and 9S3 rings, respectively (see Table 2). The Ru–S bond distances and the S–Ru–S angles in **3** and **6** are very similar, being found within the ranges 2.3396(10)–2.3851(10) Å and 85.18(4)–92.23(5)°, respectively. In comparison, the Ru–S distances in the 9S3 complexes are shorter lying in the range as follows: **8** (2.2901(18)–2.3042(12) Å) compared to 2.256(2)–2.323(2) Å for **8A** and 2.320(2)–2.329(2) Å for **4A**. The S–Ru–S angles in these 9S3 complexes are found in narrower ranges of 86.49(7)–87.29(5), 86.73(10)–89.18(8) and 86.75(9)–87.28(9)°, respectively.

The structure of **9** (Fig. 4) shows the coordination of the two thiolate S atoms of **6** to a Cp*RuCl moiety, with a mirror plane running through the atoms Ru(1), Ru(2), Cl and S(3). Considering the Cp* ligand as occupying three facial coordination sites, both metal centres are six-coordinate with an anti-prismatic arrangement of ligands. The molecule possesses a Ru–Ru bond of 2.8427 Å. This is relatively short compared to those in the two crystalline forms of **7** (2.930(1) and 3.752(1) Å, respectively) [22]. Except for the absence of a chloro ligand at Ru(2), the molecular structure of **10** (Fig. 5) is very similar to that of **9**. A pseudo-mirror plane, passing through Ru(1), Ru(2) and S(2), bisects the molecule along the Ru–Ru bond vector. The Ru–Ru bond (2.8826 Å) (Table 2) is comparable to the corresponding bond distance in **9** (2.8427 Å). In Table 2, the bond parameters of **9** and **10** are compared with those of **5**, in which a Ru–Ru bond is absent.

The microanalytical data together with the number of PF_6 counter-ions in the crystal lattice confirm that complex **6** is neutral, while **8**, **9** and **10** are monocationic, indicating oxidation states of the Ru centre as follows: **6** (+3), **8** (+2), **9** (+3, +3) and **10** (+2, +2 or +3, +1). Valence electron counts for the metal centres: **6** (17e), **8** (18e), **9** (total 36e) and **10** (total 36e) are consistent with

Table 1
Crystal and structure refinement data

Complexes	**6**	**8**	**9**	**10**
Empirical formula	$C_{14}H_{23}RuS_3$	$C_{16}H_{27}F_6PRuS_3$	$C_{24}H_{38}ClF_6PRu_2S_3$	$C_{26}H_{41}F_6PRu_2S_3$
Formula weight	388.57	561.60	805.28	796.88
Temperature (K)	293(2)	293(2)	293(2)	293(2)
Wavelength (Å)	0.71073	0.71073	0.71073	0.71073
Crystal system	Orthorhombic	Orthorhombic	Orthorhombic	Monoclinic
Space group	*Pnma*	*Pnma*	*Pbca*	$P2(1)/c$
Unit cell dimension				
a (Å)	9.8306(2)	13.0619(2)	15.2886(8)	12.7981(7)
b (Å)	14.75470(10)	11.3103(2)	16.2931(8)	13.4610(7)
c (Å)	11.4452(2)	15.2543(2)	23.9681(8)	17.7407(10)
α (°)	90	90	90	90
β (°)	90	90	90	95.174(1)
γ (°)	90	90	90	90
V (Å)	1660.10(5)	2253.58(6)	5970.4(5)	3043.8(3)
Z	4	4	8	4
D_{calc} (g cm^{-1})	1.555	1.655	1.792	1.739
Absorption coefficient (mm^{-1})	1.304	1.093	1.417	1.304
$F(000)$	796	1136	3232	1608
Crystal size (mm^3)	0.30 × 0.03 × 0.03	0.27 × 0.16 × 0.16	0.36 × 0.26 × 0.22	0.3 × 0.26 × 0.203
θ Range for data collection (°)	2.25–29.26	2.05–29.36	1.70–30.03	1.60–30.01
Index ranges	$0 \le h \le 13$, $0 \le k \le 19$, $0 \le l \le 15$	$0 \le h \le 17$, $0 \le k \le 15$, $0 \le l \le 21$	$-17 \le h \le 21$, $-22 \le k \le 22$, $-33 \le l \le 27$	$-16 \le h \le 17$, $-18 \le k \le 18$, $-19 \le l \le 24$
Reflections collected	12 701	14 696	46 015	24 178
Independent reflections	2183 [$R_{int} = 0.0699$]	3041 [$R_{int} = 0.0387$]	8595 [$R_{int} = 0.0533$]	8498 [$R_{int} = 0.0490$]
Absorption correction	SADABS	SADABS	SADABS	SADABS
Max/min transmission	0.927988 and 0.469771	0.874921 and 0.666358	0.7784 and 0.6005	0.8654 and 0.7255
Refinement method	Full-matrix least-squares on F^2	Full-matrix least-squares on F^2	Full-matrix least-squares on F^2	Full-matrix least-squares on F^2
Data/restraints/parameters	2183/3/81	3041/0/135	8595/84/343	8498/0/354
Final R indices ($I > 2\sigma(I)$)	$R_1 = 0.0469$, $wR_2 = 0.1137$	$R_1 = 0.0428$, $wR_2 = 0.1071$	$R_1 = 0.0398$, $wR_2 = 0.0902$	$R_1 = 0.0486$, $wR_2 = 0.1132$
R indices (all data)	$R_1 = 0.0772$, $wR_2 = 0.1267$	$R_1 = 0.0745$, $wR_2 = 0.1251$	$R_1 = 0.0546$, $wR_2 = 0.945$	$R_1 = 0.0664$, $wR_2 = 0.1207$
Goodness-of-fit on F^2	1.030	1.071	1.014	1.028
Largest difference peak and hole (e Å^{-3})	0.622 and −0.541	0.477 and −0.614	1.106 and −0.828	1.192 and −0.955

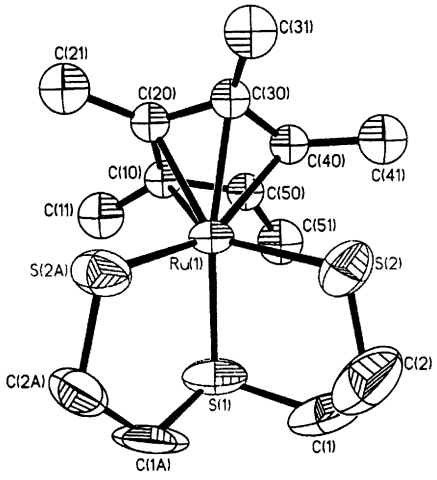

Fig. 2. ORTEP plot of **6**. Hydrogen atoms omitted for clarity. Thermal ellipsoids are drawn to 50% probability level.

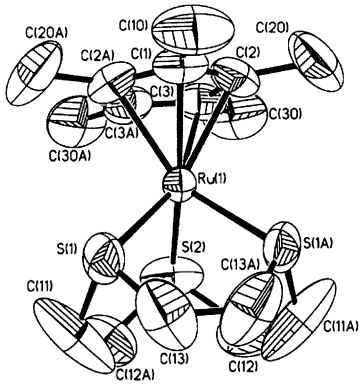

Fig. 3. ORTEP plot of the cation of **8**. Hydrogen atoms omitted for clarity. Thermal ellipsoids are drawn to 50% probability level.

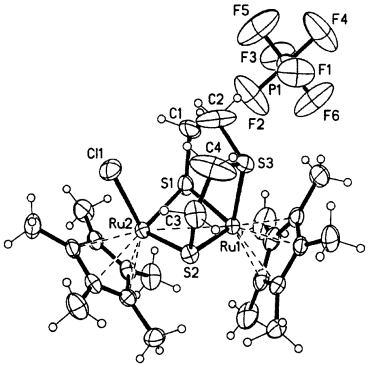

Fig. 4. ORTEP plot of the cation of **9**. Thermal ellipsoids are drawn to 50% probability level.

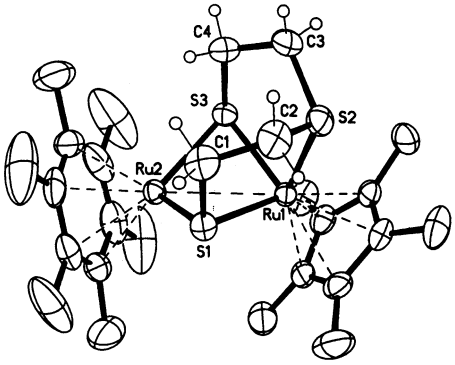

Fig. 5. ORTEP plot of the cation of **10**. Hydrogen atoms omitted for clarity. Thermal ellipsoids are drawn to 50% probability level.

the observation of the paramagnetic character of **6** and the diamagnetic character of the other complexes, as deduced from their NMR spectral characteristics.

3. Experimental

All reactions were carried out using conventional Schlenk techniques under an inert atmosphere of nitrogen or under argon in an M. Braun Labmaster 130 Inert Gas System.

NMR spectra were measured on a Bruker 300 or 500 MHz FT NMR spectrometer; for ^{1}H and ^{13}C spectra, chemical shifts were referenced to residual solvent in the deutero-solvents—$CDCl_3$, CD_2Cl_2, C_6D_6, and $C_6D_5CD_3$. IR spectra in KBr pellets or Nujol mulls were measured in the range 4000–200 cm^{-1} by means of a BioRad FTS-165 FTIR instrument. Mass spectra were run on a Finnigan Mat 95XL-T (FAB) or a Finnigan-MAT LCQ (ESI) spectrometer. Elemental analyses were performed by the microanalytical laboratory in-house. Cyclic voltammetry was carried out in CH_3CN using a double glassy carbon electrode with a Ag^{+} (0.010 M $AgNO_3$, 0.10 M $N(Bu^n)_4BF_4$ reference electrode. A 0.1 M solution of $N(Bu^n)_4BF_4$ was used as a supporting electrolyte. Electrochemical measurements were performed on an Elechema PS-605 Potentiostat/FG-206F Waveform Generator combination (Elechema, Potsdam, NY, USA) and the results recorded on a Graphtec WX2400 x–y recorder (Graphtec Corporation, Tokyo Japan). $((C_6Me_6)RuCl_2)_2$ (**2**) and $[Cp^*RuCl_2]_2$ (**7**) were synthesised from $RuCl_3 \cdot nH_2O$ (Oxkem) as described in the literature [23,24]. All solvents were dried over sodium/benzophenone and distilled before use. Celite (Fluka AG), silica gel (Merck Kieselgel 60, 230–400 Mesh) were dried at 140 °C overnight before chromatographic use.

Table 2
Selected bond parameters (bond lengths in Å; bond angles in (°))

	3	**6** [a]	**4A**	**8**	**8A**	**5**	**9**	**10**
Bond lengths								
Ru(1)–S(1)	2.3396(10)	2.3409(12)	2.320(2)	2.3042(12)	2.256(2)	2.3672(19)	2.3004(8)	2.3465(10)
Ru(1)–S(2)	2.3851(10)	2.3850(12)	2.323(2)	2.2901(18)	2.323(2)	2.3653(19)	2.2953(8)	2.3151(10)
Ru(1)–S(3)	2.3807(10)	2.3808(12)	2.329(2)	2.3042(12)	2.288(2)	2.3032(19)	2.2937(9)	2.3312(10)
Ru(2)–S(1)	–	–	–	–	–	2.415(2)	2.3197(8)	2.3134(9)
Ru(2)–S(2)	–	–	–	–	–	2.414(2)	2.3121(8)	–
Ru(2)–S(3)	–	–	–	–	–	–	–	2.3019(10)
Ru(1)–Ru(2)	–	–	–	–	–	3.71 [b]	2.8427(3)	2.8826(4)
Bond angles								
S(2)–Ru)(1)–S(1)	85.18(4)	85.22(5	87.28(9)	87.29(6)	88.39(8)	79.09(7	101.57(3)	86.77(4)
S(2)–Ru(1)–S(3)	92.18(4)	92.23(5)	87.05(9)	87.29(5)	89.18(8)	86.16(7)	86.34(3)	86.50(4)
S(1)–Ru(1)–S(3)	85.41(4)	85.40(4)	86.75(9)	86.49(7)	86.73(10)	86.17(7)	87.01(3)	90.12(3)
S(1)–Ru(2)–S(2)	–	–	–	–	–	77.22(7)	100.48(3)	–
S(1)–Ru(2)–S(3))	–	–	–	–	–	–	–	91.69(3)

[a] For complex **6**, S(3) is labeled as S(2A).
[b] Ru···Ru non-bonding distance.

3.1. Synthesis of η^5-pentamethylcyclopentadienyl 3-thiapentane-1,5-dithiolate ruthenium(III), $Cp^*Ru[S((CH_2)_2S)_2]$ (6)

To a suspension of sodium methoxide (freshly generated from sodium (17.8 mg, 7.74 mmol)) in THF (20 ml) was injected 2-mercaptoethyl sulfide (0.51 ml, 3.91 mmol) and the mixture stirred overnight. To the gel-like suspension was added $[(Cp^*RuCl_2)_2]$ (**7**) (1.20 g, 1.95 mmol) as a solid; the suspension turned purple instantaneously. The mixture was allowed to stir at ambient temperature for 24 h, and then filtered via a cannula to remove white solids of NaCl. The purple filtrate was evacuated to dryness and the residue dissolved in a 1:1 toluene–ether mixture (ca. 10 ml) and then loaded on a silica gel column (15×1 cm) packed in hexane. A purple band was eluted with 1:1 toluene–ether (ca. 50 ml), which upon concentration and addition of ether yielded lustrous dark purple needles of [Cp*Ru(tpdt)] (**6**) (0.59 g, 1.51 mmol, 40% yield) after 10 h at -30 °C, followed by subsequent crops (total 0.25 g, 0.64 mmol, 17% yield). Diffraction-quality crystals were selected from the crops of crystals obtained above. Anal. Found: C, 43.3; H, 6.0; S, 24.3. Calc for $C_{14}H_{23}S_3Ru$: C, 43.3; H, 6.0; S, 24.8%. ^{1}H-VT-NMR (500 MHz, $CDCl_3$): 300 K δ -0.10 (br s, $v_{1/2}$ ca. 50 Hz), -3.15 (br s, $v_{1/2}$ ca. 200 Hz); 237 K δ -3.77 (v br s, $v_{1/2}$ ca. 250 Hz), 0.71 (br s, $v_{1/2}$ ca. 50 Hz); 253 K δ -4.49 (v br s, $v_{1/2}$ ca. 450 Hz), -1.81 (v br s, $v_{1/2}$ ca. 175 Hz); 233 K δ -5.2 (v br s, $v_{1/2}$ ca. 600 Hz), 213 and 193 K no signals. IR (KBr, cm^{-1}): v 2968m, sh, 2906vs, 2816m sh, 2363m, 2343m, 1458m, 1398m, 1374m, 1268w, 1225w, 1149vvw sh, 1101w, 1085w, 1025m, 909w, 836m, 817vw, 765vvw, 749vvw, 669w. FAB$^+$-MS: m/z 389 ($Cp^*Ru(S(CH_2)_2)_2S$); FAB$^-$-MS: m/z 145 (PF_6).

3.2. Synthesis of η^5-pentamethylcyclopentadienyl ruthenium(II) 1,4,7 trithiacyclononane hexafluorophosphate, $[Cp^*Ru(9S3)](PF_6)$ (8)

To a stirred suspension of $[(Cp^*RuCl_2)_2]$ (**7**) (1.010 g, 1.64 mmol) in acetone (10 ml) was added solid $AgPF_6$ (1.66 g, 6.57 mmol). A red–brown mixture was formed immediately with precipitation of AgCl, which was removed by filtration through a disk of Celite (1.5×1 cm^2). To the dark red–brown filtrate was added solid 9S3 (0.592 g, 3.28 mmol) and the suspension stirred overnight (20 h), giving a yellowish brown solution. Filtration through a disc of alumina (3×1 cm^2) removed a gummy brown solid giving a bright yellow solution. Concentration and addition of ether yielded bright yellow prisms of [Cp*Ru(9S3)](PF_6) (**8**) (0.28 g, 0.50 mmol, 15% yield) after 15 h at -30 °C, followed by subsequent crops (total 0.51 g, 27% yield) and an unknown orange solid (5 mg). Diffraction-quality crystals were selected from the fast crop. Anal. Found: C, 34.7; H, 5.5; P, 4.7; S, 17.5. Calc. for $C_{16}H_{27}F_6PS_3Ru$: C, 34.2; H, 4.8; P, 5.5; S, 17.1%. ^{1}H-NMR (500 MHz, $CDCl_3$): δ 2.42 (m, 12H, CH_2), 1.78 (s, 15H, $C_5(CH_3)_5$); ^{13}C and ^{13}C-DEPT135 NMR (75 MHz, $CDCl_3$): δ 91.2 (C_5Me_5), 34.2 (CH_2), 9.9 ($C_5(CH_3)_5$). IR (KBr, cm^{-1}): v 2976w, 2916m, 2855m, 2370m, 2346m, 1456m, 1411m, 1386m, 1128vvw, 1080vw, 1030w, 837vvs (PF_6), 557s (PF_6). FAB$^+$-MS: m/z 417 (Cp*Ru9S3); FAB$^-$-MS: m/z 145 (PF_6). Cyclic voltammetry: 0.1 mM of **2** in 1.0 M of $[N(Bu^t)_4][BF_4]/CH_3CN$ supporting electrolyte solution at $I = 100$ μA full scale. Oxidation: scan rate = 100 mV s^{-1}, $X = 200$ mV cm^{-1}, $Y = 50$ mV cm^{-1}, $E_{1/2} = +0.713$ mV. Reduction: scan rate = 100 mV s^{-1}, $X = 200$ mV cm^{-1}, $Y = 50$ mV cm^{-1}, $I = 100$ μA full scale, $E_{pc} = -3.00$ V.

3.3. Reaction of $Cp^*Ru(tpdt)$ (6) with $[(Cp^*RuCl_2)_2]$ (7)

The complex **7** (16 mg, 0.026 mmol) was added as a solid to a stirred purple solution of **6** (20 mg, 0.051 mmol) in acetone (10 ml). The solution changed to dark yellow within 10 min; after 4 h at ambient temperature, solid NH_4PF_6 (33 mg, 0.20 mmol) was added and the precipitated NH_4Cl removed by filtration through a disk of Celite (1.5×1 cm^2). Concentration of the yellow filtrate followed by addition of ether gave very fine plate-like dark red crystals of [Cp*Ru(tpdt)Ru(Cl)Cp*](PF_6) (**9**) (28 mg, 0.035 mmol, 70% yield). Diffusion of ether into a CH_2Cl_2 solution of **9** for 2 weeks at -30 °C gave diffraction-quality thick red columnar crystals. Anal. Found: C, 35.9; H, 4.8; Cl, 4.5; S, 12.2; Ru, 25.6. Calc. for $C_{24}H_{38}ClF_6PS_3Ru_2$: C, 35.8; H, 4.8; Cl, 4.4; S, 11.9; Ru, 25.1%. ^{1}H-NMR (300 MHz, $CDCl_3$): δ 1.65 (s, 15H, $C_5(CH_3)_5$), 1.88 (s, 15H, $C_5(CH_3)_5$), 2.69–2.79 (m, 2H, CH_2), 2.92–3.13 (m, 6H, $3CH_2$); ^{13}C-NMR (75 MHz, $CDCl_3$): δ 10.0 and 10.7 ($C_5(CH_3)_5$), 37.4 and 41.6 (CH_2), 101.2 and 102.4 ($C_5(CH_3)_5$). IR (KBr, cm^{-1}): v 3013m, 2981m, 2965m, 2916s, 2852w, sh, 1485s, 1465m, 1453m, 1427s, 1376s, 1291vw, 1259vw, 1157vw, 1141vvw, 1073s, 1027s, 840vvs (PF_6), 678vw, 619w, 557vs (PF_6). ESI$^+$-MS: m/z 661 {$Cp^*Ru((S(CH_2)_2)_2S)Ru(Cl)Cp^*$}, 625 {$Cp^*Ru((S(CH_2)_2)_2S)RuCp^*$}, 597 ($Cp^*Ru(S(CH_2)_2S_2)RuCp^*$), 569 ($Cp^*Ru(S_3)RuCp^*$}, 537 ($Cp^*Ru(S_2)RuCp^*$}; ESI$^-$-MS: m/z 145 (PF_6).

3.4. Reaction of $[Cp^*Ru(tpdt)]$ (6) with $[(C_6Me_6)RuCl_2]_2$ (2)

Orange solids of $[(C_6Me_6)RuCl_2]_2$ (**2**) (43 mg, 0.064 mmol) was added to a stirred purple solution of **6** (50 mg, 0.13 mmol) in acetone (10 ml). A dark brown–green suspension formed almost instantaneously and the reaction mixture was allowed to stir at ambient tem-

perature for 1.5 h. Filtration of the resulting product mixture through a glass-sinter removed some unreacted solid (20 mg) of **2**. To the deep brown–green solution was added solid NH_4PF_6 (0.11 g, 0.68 mmol), and the precipitated NH_4Cl removed by filtration through a disc of Celite (1.5×1 cm^2) to give a brownish green solution. Concentration followed by addition of ether gave fine purplish red solids of [Cp*Ru(tpdt)Ru(C_6Me_6)](PF_6) (**10**) (8 mg, 0.010 mmol, 8%). Elution of the mother liquor through a silica-gel column (5 mm × 5 cm) using a mixture of THF and acetone (1:1, ca. 15 ml) gave a dark purplish-red solution which gave thin plate-like crystals of **10** (17 mg, 17%), followed by a dark green band which gave trace amounts of an intractable mixture (< 1%). Diffusion of ether into a CH_2Cl_2 solution of **10** for 2 weeks at −30 °C gave diffraction-quality thick purple needles. Anal. Found: C, 39.6; H, 5.4; P, 3.2; S, 11.5; Calc. for $C_{26}H_{41}F_6PS_3Ru_2$: C, 39.2; H, 5.2; P, 3.9; S, 12.1%. ^{1}H-NMR (300 MHz, $CDCl_3$): δ 0.75 (m, 2H, CH_2), 1.72 (s, 15H, $C_5(CH_3)_5$), 1.92 (m, 2H, CH_2), 2.25 (s, 18H, $C_6(CH_3)_6$), 3.03–3.27 (m, 4H, $(CH_2)_2$); ^{13}C-NMR (75 MHz, $CDCl_3$): δ 6.1 ($C_5(CH_3)_5$), 12.8 ($C_6(CH_3)_6$), 32.5 and 41.3 (CH_2), 88.7 ($C_6(CH_3)_6$), 91.0 ($C_5(CH_3)_5$). IR (KBr, cm^{-1}): ν 2965w, 2911s, 2852w, sh, 1447w, 1415vw, 1388s, 1130w, sh, 1097w, 1065m, 1010s, 839vvs (PF_6), 557vs (PF_6). ESI$^+$-MS: *m/z* 653 {Cp*Ru($(S(CH_2)_2)_2S$)Ru(C_6Me_6)), 625 {Cp*Ru($S(CH_2)_2S_2$)Ru(C_6Me_6)}, 596 {Cp*Ru(S_3)Ru(C_6Me_6)}, 564 {Cp*Ru(S_2)Ru(C_6Me_6)}, 434 {Ru(S_2)-Ru(C_6Me_6)}; ESI$^-$-MS: *m/z* 145 (PF_6).

3.5. Structure determinations

Crystals were mounted on quartz fibres. X-ray data were collected on a Siemens SMART CCD system, using Mo–K_α radiation. Data were corrected for Lp with the SMART suite of programs [25], and for absorption effects with SADABS [26]. Structural solution and refinement were carried out with the SHELXTL suite of programs [27].

The structures were solved by direct methods to locate the heavy atoms, followed by difference maps for the lighter non-hydrogen atoms. Hydrogen atoms were placed in calculated positions and refined with a riding model. With the exception of those mentioned below, all non-hydrogen atoms were given anisotropic thermal parameters in the final model.

The Cp* ring in **6** exhibited disorder. This was modeled with two alternative sites, with occupancies summed to unity. A common isotropic thermal parameter was employed for all the ring carbon atoms, and another for all the methyl carbons. The 9S3 ligand was also disordered over two alternative sites, with equal occupancies; the corresponding bond lengths for the two sites were restrained to be the same.

4. Conclusion

The complexes [Cp*Ru(tpdt)] (**6**) and [Cp*Ru-(9S3)](PF_6) (**8**) were obtained from [(Cp*$RuCl_2)_2$] (**7**). The interaction of **6** with **7** and [(C_6Me_6)$RuCl_2]_2$ (**2**) led to the isolation of M–M bonded dinuclear species **9** and **10**, respectively.

5. Supplementary material

Crystallographic data for the structural analyses has been deposited with the Cambridge Crystallographic Data Centre, CCDC no. 188513–16 for compounds **6**, **8**, **9**, **10**. Copies of this information may be obtained free of charge from The Director, CCDC, 12 Union Road, Cambridge, CB2 1EZ, UK [fax. (int code): +44-1223-336-033, or e-mail: deposit@ccdc.cam.ac.uk or www: http://www.ccdc.cam.ac.uk)

Acknowledgements

Support from the National University of Singapore under Academic Research Fund grant no. R-143-000-046-112 and a Research Scholarship to MET is gratefully acknowledged.

References

[1] (a) E.I. Stiefel, K. Matsumoto (eds.), Transition Metal Sulfur Chemistry—Biological and Industrial Significance, ACS Symposium Series 653, 1996;
(b) I. Dance, K. Fisher, Prog. Inorg. Chem. 41 (1994) 637;
(c) T. Shibahara, Coord. Chem. Rev. 123 (1993) 73;
(d) R.H. Holm, S. Ciurli, J.A. Weigel, Prog. Inorg. Chem. 38 (1990) 1;
(e) P. Mathur, Adv. Organomet. Chem. 41 (1997) 243;
(f) H. Orgino, S. Inomata, H. Tobita, Chem. Rev. 98 (1998) 2093;
(g) J.B. Howard, D.C. Rees, Chem. Rev. 96 (1996) 2965;
(h) D. Sellman, J. Sutter, Acc. Chem. Res. 30 (1997) 460;
(i) R.A. Sanchez-Delgado, J. Mol. Catal. 86 (1994) 287;
(j) M.D. Curtis, S.H. Druker, J. Am. Chem. Soc. 119 (1997) 1027;
(k) C. Bianchini, A. Meli, Acc. Chem. Res. 31 (1998) 109 (and references therein);
(l) B.K. Burgess, D.J. Lowe, Chem. Rev. 96 (1996) 2983.
[2] A. Müller, E. Diemann, in: G. Wilkinson, R.D. Gillard, J.A. McCleverty (Eds.), Comprehensive Coordination Chemistry, vol. 2 (Chapter 16.1), Pergamon Press, Oxford, 1987.
[3] K.P. Maresca, F.J. Femia, G.H. Bonavia, J.W. Babich, J. Zubieta, Inorg. Chim. Acta 297 (2000) 98.
[4] K.P. Maresca, G.H. Bonavia, J.W. Babich, J. Zubieta, Inorg. Chim. Acta 284 (1999) 252.
[5] T. Fietz, H. Spies, H.-J. Pietzsch, P. Leibnitz, Inorg. Chim. Acta 231 (1995) 233.
[6] H.-J. Pietzsch, H. Spies, S. Hoffmann, Inorg. Chim. Acta 165 (1989) 163.
[7] H. Spies, T. Fietz, H.-J. Pietzsch, B. Johannsen, P. Leibnitz, G. Reck, D. Scheller, K. Klostermann, J. Chem. Soc. Dalton Trans. (1995) 2277.

[8] G.E.D. Mullen, P.J. Blower, D.J. Price, A.K. Powell, M.J. Howard, M.J. Went, Inorg. Chem. 39 (2000) 4093.
[9] J.-H. Kim, J.-W. Hwang, Y.-W. Park, Y. Do, Inorg. Chem. 38 (1999) 353.
[10] M.-A. Munoz-Hernández, R. Cea-Olivares, R.-A. Toscano, S. Hernández-Ortega, Z. Anorg. Allg. Chem. 623 (1997) 642.
[11] (a) K. Tatsumi, Y. Sekiguchi, A. Nakamura, J. Am. Chem. Soc. 103 (1986) 1358;
(b) H. Kawaguchi, K. Tatsumi, A. Nakamura, J. Chem. Soc. Chem. Commun. (1995) 111.
[12] R.Y.C. Shin, M.A. Bennett, L.Y. Goh, W. Chen, D.C.R. Hockless, W.K. Leong, K. Mashima, A.C. Willis, Accepted for Inorg. Chem.
[13] D. Sellmann, L. Zapf, J. Organomet. Chem. 289 (1985) 51.
[14] M.A. Bennett, L.Y. Goh, A.C. Willis, J. Am. Chem. Soc. 118 (1996) 4984.
[15] G.J. Grant, T. Salupo-Bryant, L.A. Holt, D.Y. Morrissey, M.J. Gray, J.D. Zubkowski, E.J. Valente, L.F.J. Mehne, J. Organomet. Chem. 587 (1999) 207.
[16] (a) L.Y. Goh, W.K. Leong, P.H. Leung, Z.Q. Weng, I. Haiduc, J. Organomet. Chem. 607 (2000) 64;
(b) L.Y. Goh, Y.Y. Lim, J. Organomet. Chem. 402 (1991) 209;
(c) L.Y. Goh, S.K. Khoo, Y.Y. Lim, J. Organomet. Chem. 399 (1990) 115.
[17] (a) A.J. Blake, R.D. Crofts, G. Ried, M. Schröder, J. Organomet. Chem. 359 (1989) 371;
(b) A.J. Blake, R.O. Gould, A.J. Holder, T.I. Hyde, M. Schröder, J. Chem. Soc. Dalton Trans. (1988) 1861.
[18] M.N. Bell, A.J. Blake, R.M. Christie, R.O. Gould, A.J. Holder, T.I. Hyde, M. Schröder, L.J. Yellowlees, J. Chem. Soc. Dalton Trans. (1992) 2977.
[19] (a) S.C. Rawle, S.R. Cooper, Inorg. Chem. 26 (1987) 3769;
(b) M.N. Bell, A.J. Blake, M. Schröder, H.-J. Küppers, K. Wieghardt, Angew. Chem. Int. Ed. Engl. 26 (1987) 250;
(c) M.N. Bell, A.J. Blake, A.J. Holder, T.I. Hyde, M. Schröder, L.J. Yellowlees, J. Chem. Soc. Chem. Commun. (1992) 848.
[20] D.T. Sawyer, A. Sobkowiak, J.L. Roberts, Electrochemistry for Chemists, 2nd ed., Wiley-Interscience, New York, 1995, pp. 201–202.
[21] S.R. Cooper, S.C. Rawle, Struct. Bonding 72 (1990) 1.
[22] U. Koelle, J. Kossakowski, N. Klaff, L. Wesemann, U. Enghert, G.E. Heberich, Angew. Chem. Int. Ed. Engl. 30 (1991) 690.
[23] U Koelle, J. Kossakowski, Inorg. Synth. 29 (1992) 225.
[24] M.A. Bennett, T.-N. Huang, T.W. Matheson, A.K. Smith, Inorg. Synth. 21 (1982) 74.
[25] SMART version 4.05, Siemens Energy & Automation Inc., Madison, Wisconsin, USA.
[26] G.M. Sheldrick, SADABS, 1996.
[27] SHELXTL version 5.03, Siemens Energy & Automation Inc., Madison, Wisconsin, USA.